Journal of Magnetic Resonance 310 (2020) 106656

Contents lists available at ScienceDirect

Journal of Magnetic Resonance

journal homepage: www.elsevier.com/locate/jmr

Rapid-melt DNP for multidimensional and heteronuclear high-field NMR experiments

S.G.J. van Meerten, G.E. Janssen, A.P.M. Kentgens *

Magnetic Resonance Research Center, Institute for Molecules and Materials, Radboud University, Nijmegen, the Netherlands

ARTICLE INFO

Article history:
Received 10 September 2019
Revised 14 November 2019
Accepted 15 November 2019
Available online 25 November 2019

Keywords:
Nuclear magnetic resonance
NMR
Dynamic nuclear polarization
DNP
Rapid melt
Multidimensional
Stripline NMR

ABSTRACT

Low sensitivity is the main limitation of NMR for efficient chemical analysis of mass-limited samples. Hyperpolarization techniques such as Dynamic Nuclear Polarization (DNP) have greatly improved the efficiency of NMR experiments. In this manuscript, we demonstrate a 400 MHz rapid-melt DNP setup. With this setup it is possible to perform liquid-state NMR experiments with solid-state DNP enhancement at high magnetic field. Sample volumes of 100 nL in fused-silica capillaries are detected using a stripline microcoil. Due to the small heat capacity of these samples it is possible to melt them with relatively low relaxation losses. With this 400 MHz setup, proton enhancements of up to −175 have been obtained in the liquid-state. The probe is double tuned, so it can be used for heteronuclear DNP-NMR and since the sample composition does not change during the experiment, it is possible to perform signal averaging and multidimensional experiments. This type of rapid-melt DNP setup thus allows for most types of liquid-state NMR experiments to be combined with efficient solid-state DNP. This makes rapid-melt DNP an interesting method for high-throughput chemical analysis of mass-limited samples.

1. Introduction

Nuclear Magnetic Resonance is a powerful method for chemical analysis as it provides detailed information on structure and dynamics. It is, however, limited by sensitivity. To overcome this limitation, hyperpolarization techniques such as Dynamic Nuclear Polarization (DNP) have been developed [1] and have gained in popularity in recent years. These hyperpolarization techniques could greatly improve the efficiency of chemical analysis using NMR.

Currently, the highest levels of DNP hyperpolarization in the liquid state are achieved by dissolution DNP [2]. With this method, polarization levels of up to 70% have been reached for ^{13}C [3]. At the moment, the main application of this technique is to generate hyperpolarized ^{13}C-pyruvate for pre-clinical and clinical studies using MRI [4]. Dissolution DNP is, however, not particularly suitable for chemical analysis of mass-limited samples. Firstly, the polarization buildup times are quite long, in the order of an hour. This severely limits the throughput of this method. And secondly, dissolution DNP is a "single shot" method. After the experiment, the sample has been diluted and any repetition of the experiment requires fresh sample. This makes the method quite sensitive to experimental issues, which could result in loss of sample. Also, any multidimensional experiment can only be recorded using an Ultrafast method [5]. All these issues limit the application of dissolution DNP to high-throughput NMR analysis.

Another interesting method to obtain high NMR signal enhancements in the liquid state is to perform DNP on a frozen sample and then melt it within the longitudinal relaxation time. This can be done using an infrared laser [6,7] or with high power microwaves generated by a gyrotron [8]. In our lab, a rapid-melt setup has been developed, which combines the high enhancements of solid state DNP with the high resolution of liquid state NMR without changing the sample composition [9]. The technique works by hyperpolarizing a frozen sample using a solid state DNP mechanism (e.g., solid effect) and then rapidly melting the sample within the relaxation time of the nuclear spins. This technique is enabled by a stripline NMR detector [10], which has a detection volume in the order of 100 nL, together with capillary sized samples. The stripline detector has a limit of detection in the order of 10^{14} H^1 spins per square-root hertz. For a thorough discussion on the stripline design, the reader is referred to the article by Bart et al. [11]. Since the sample volumes are small, the heat capacity is low and thus the sample can be melted efficiently and in a reproducible way. The rapid-melt DNP setup is flexible and can be used to investigate the various DNP mechanisms

* Corresponding author at: Magnetic Resonance Research Center, Heyendaalseweg 135, 6525 AJ Nijmegen, the Netherlands.
E-mail address: a.kentgens@nmr.ru.nl (A.P.M. Kentgens).

https://doi.org/10.1016/j.jmr.2019.106656
1090-7807/

conveniently, both in the solid state and in the liquid state [12]. In this manuscript, we present the developments of a 9.4 T, double channel rapid-melt DNP probe, which can be used to perform multidimensional liquid state NMR experiments with the increased sensitivity offered by hyperpolarizing the spin system in the solid-state.

2. Experimental

Fig. 1 shows a schematic of the 9.4 T rapid-melt setup. In this setup, a 350 μm outer diameter, 150 μm inner diameter, fused-silica capillary contains the sample. The sample is located at the bottom end of the capillary. The capillary is then sealed at both ends. At the top, this capillary is clamped to a fiberglass rod, which runs all the way through the probe. Outside of the NMR magnet, the rod is attached to a linear motor (LinMot), which moves the sample to the different locations. During a rapid-melt measurement, the sample moves to three positions in the NMR probe. A fixed 700 μm outer diameter, 500 μm inner diameter, capillary guides the moving sample capillary. This guiding capillary runs from the top of the stripline detector to the top of the melt area. This is shown in Fig. 3. Fitting the stripline with the larger guiding capillary does, however, results in a lower sensitivity. The stripline detector for a 700 μm capillary has a sensitivity of 75% compared to that for a 350 μm capillary.

Fig. 2 shows a drawing of the cryogenic and heating system. The experiment starts with the sample located in the DNP area which has a small chamber filled with liquid nitrogen. This liquid nitrogen is used to freeze the sample and keep it cold during the DNP. The nitrogen is continuously replenished through the inlet by a transfer line (Cryogenic Ltd.) connected to a nitrogen dewar

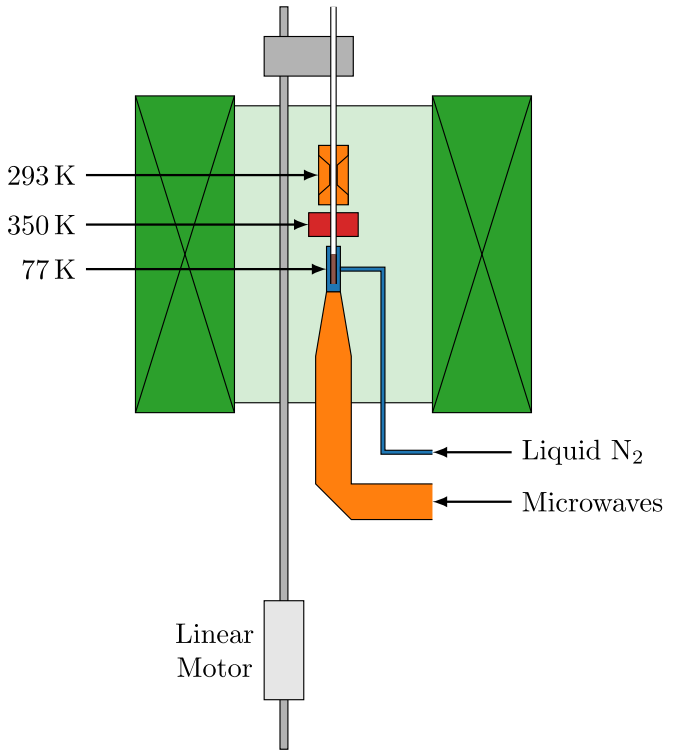

Fig. 1. Schematic of the rapid-melt system. The setup has three distinct areas. From bottom to top: the freeze/DNP area, the melt area, and the NMR stripline detector. A linear motor moves the sample to the three locations. The schematic shows the system with the sample in the DNP position.

pressurized to approximately 0.1 bar overpressure. The evaporating nitrogen leaves through an exhaust located above the DNP area. The exhaust consists of two concentric pipes. The cold nitrogen flows down through the copper inner exhaust, while a hot nitrogen gas flow upwards through the outer fiberglass pipe prevents the probe from becoming too cold. In addition, the copper pipe is heated electrically to further stabilize the temperature of the probe.

Inside the DNP area, the frozen sample is irradiated with microwaves. The microwaves are generated by an extended interaction klystron oscillator (CPI), which has a power output of approximately 4 W. The klystron is tuned mechanically to set the microwave frequency for optimal solid effect DNP. Fine-tuning of the frequency is done by slight adjustments of the klystron's cathode voltage. An oversize ($d = 10$ mm) circular waveguide guides the microwaves from the klystron to the DNP area in the probe. The waveguide tapers down to a diameter of 1.2 mm before entering the DNP area. A Mylar film, fixed between the waveguide flanges, prevents the cryogens from flowing down the waveguide.

After polarizing the sample in the DNP area, it moves up to the melt area. The melt area consists of a copper "block". This melting-block is a cylinder with a diameter of 6 mm, a height of 10 mm, and a hole of 400 μm through which the capillary moves. This copper block is heated electrically. Because of the relatively small distance between the melt area and the NMR detector, the electrical heater is located lower in the probe. This prevents the electrical circuit of the heater from generating noise in the stripline detector. A copper heat pipe connects the electrical heater to the melting-block. The temperature of the melting-block can be regulated and set to a value high enough to melt the sample quickly, but not so high as to create gas bubbles in the sample. This means that with a sample like water or toluene, the temperature of the melting-block can be higher than, for example, with methanol. Due to the small volume and thus the low heat capacity, the sample melts rapidly. This means relaxation losses during melting are relatively limited.

After the sample has melted, it moves up to the stripline for NMR detection. The stripline chip is 25 mm long and 10 mm wide. The sensitive region of the strip has a width of 0.5 mm and has a length of 8 mm. The probe is double resonant for ^{1}H (397 MHz) and ^{13}C (100 MHz). A nitrogen gas flow keeps the NMR detector at room temperature. A Shim-on-Chip [13] system homogenizes the magnetic field inside the stripline detector. All experiments were performed on a 9.4 T magnet (Agilent) with a Varian Infinity Plus Spectrometer running SpinSight software (Varian), the data was processed using ssNake [14].

The shuttling and positioning is controlled using the PID in the servo controller (LinMot). The distance between the DNP and the melting-block is 34 mm and the distance between the melting-block and the center of the NMR detector is 25 mm. Shuttling between two locations takes approximately 75 ms (130 ms for shuttling directly between the DNP and NMR locations), this includes the time it takes the capillary/sample to settle in the final position. Since the sample composition does not change during the experiment, the entire process of hyperpolarization, melting and NMR acquisition is repeatable. This is used for signal averaging, but more importantly, it is used to record the increments of a multidimensional NMR spectrum. Since the detector is double resonant, it is possible to perform both homonuclear and heteronuclear experiments with this type of probe.

Regularly, the capillary used in rapid-melt experiments is sealed at both ends. It is, however, possible to perform stopped-flow experiments using this type of setup. For this purpose, we have created a concentric flow design, of which a diagram is shown in Fig. 4. The design consists of two capillaries, an outer capillary (350 μm O.D., 200 μm I.D.) and an inner capillary (160 μm O.D.,

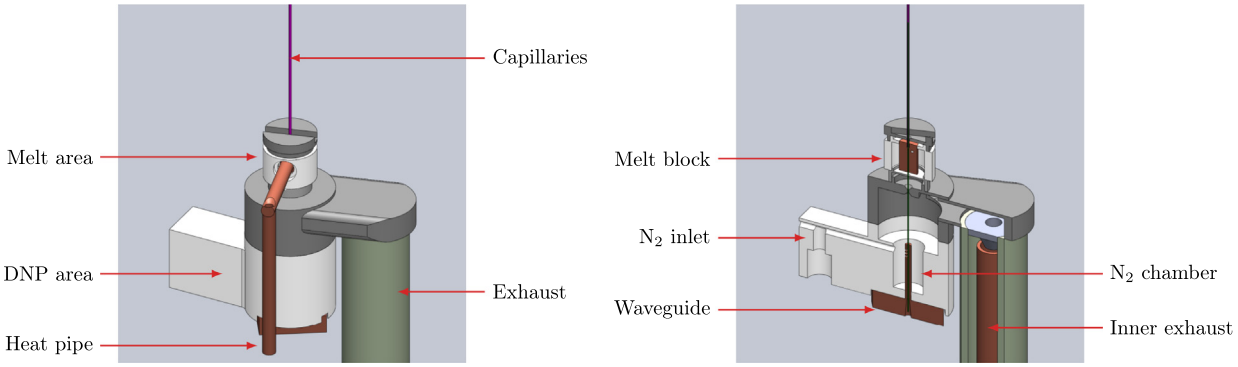

Fig. 2. Schematic of the cryogenic and melt areas of the rapid-melt probe. The waveguide taper, the nitrogen transfer line, and the electric heater are not shown here. Also, the protective cover of the heat pipe and the insulation surrounding the waveguide has been omitted. The stripline detector is positioned directly above the melting-block.

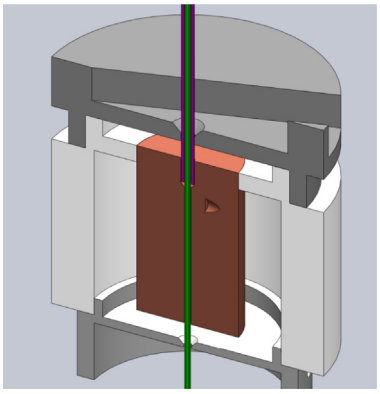

Fig. 3. Schematic of the melt area of the rapid-melt probe. In purple, the static guidance capillary is shown. In green, the sample capillary is shown.

100 µm I.D.). The outer capillary is sealed with a piece of fused silica fixed into the bottom of the capillary with polyimide resin or UV curable glue. The two concentric capillaries replace the single sample capillary and move through the guiding capillary to the three locations in the probe. Located at the top of the probe is a T-junction through which the sample enters by flow via the inner capillary and exits from the space in between the two capillaries. When the sample has melted and moved to the NMR position, all the material inside the capillaries will be in the liquid state. It is then possible to replace the sample by a flow of liquid. Such a method is thus well suited for stopped-flow in-line experiments, it does, however, reduce the sample volume to 65% compared to a single capillary measurement.

3. Results

3.1. ^{1}H DNP-NMR

To demonstrate the 400 MHz rapid-melt DNP setup, a sample of 500 mM ^{13}C-toluene in toluene-d_8 with a radical concentration of approximately 80 mM BDPA was used. The sample was sealed inside a piece of capillary using UV curable glue. The proton T_1 relaxation time of the sample was 600 ms (a sample without radicals has a T_1 in the order of 5 s). A broadening of the resonances by the radical is not observed due to the linewidths achieved in the rapid melt DNP setup (20 Hz FWHM).

In the DNP experiment, the sample was polarized for 10 s and melted/shuttled in 0.3 s. For reference, the thermal spectrum was recorded without any shuttling. This resulted in the spectra shown in Fig. 5, both of which were recorded in a single scan. The enhancement factor is approximately −175 with respect to a thermal experiment and is comparable for all proton resonances.

Fig. 6a shows the enhancement as a function of the polarization time t_{DNP} and Fig. 6b shows the enhancement as a function of the melting time t_{melt}, which includes the shuttling time of 150 ms. The enhancement is determined by integrating the full spectrum with a spectral width of 10 kHz. Before 0.2 s, the signals are broader than the spectral width of the spectrum, as the sample has not yet completely melted. After approximately 0.3 s, the resonances reach a linewidth comparable to the thermal spectrum.

(a) Bottom (b) Top

Fig. 4. Schematics of the concentric capillaries for stopped-flow experiments. At the bottom (a), the outer capillary is closed with glue (shown in red). At the top (b), a T-junction separates the inwards and outwards flow. (For interpretation of the references to colour in this figure legend, the reader is referred to the web version of this article.)

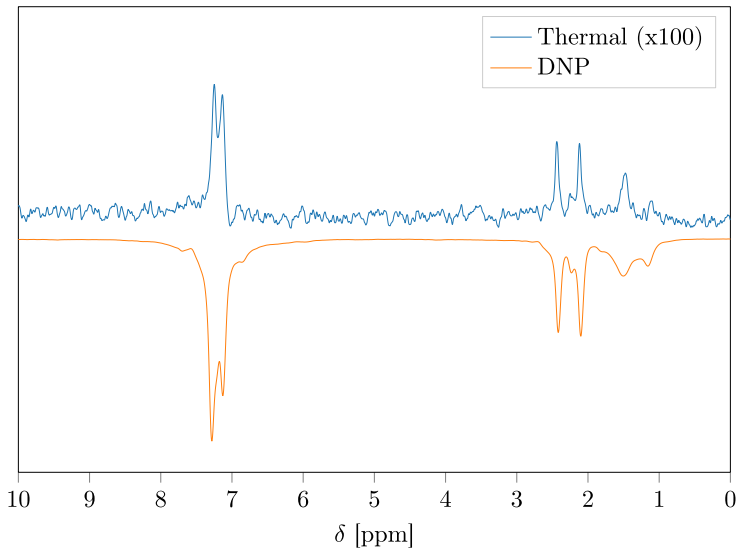

Fig. 5. ^{1}H spectra of 500 mM ^{13}C-toluene mixed with toluene-d_8 together with approximately 80 mM BDPA. The enhancement factor is −175 with respect to the thermal signal.

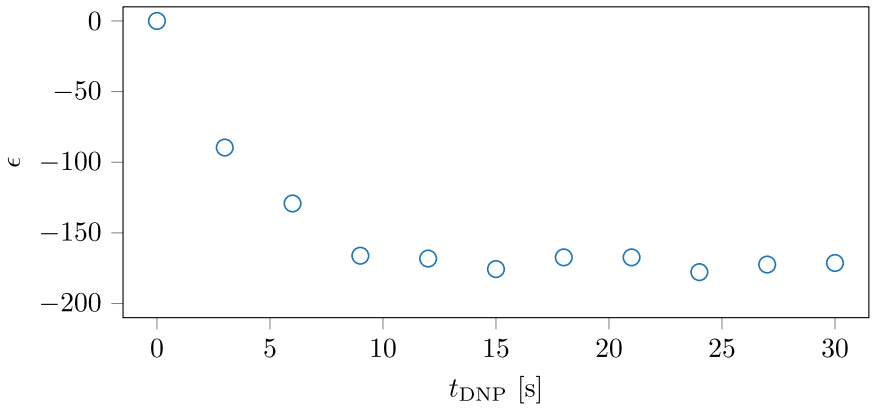

(a) Buildup curve

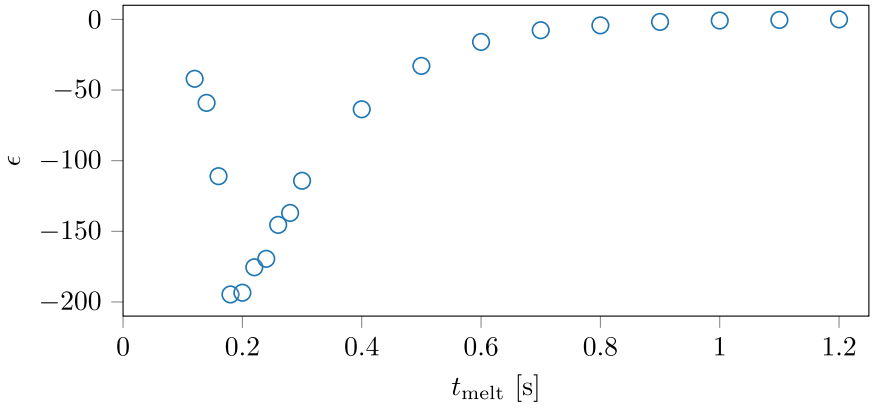

(b) Melting curve

Fig. 6. The ^{1}H buildup and melting curves of 500 mM ^{13}C-toluene in toluene-d_8 together with approximately 80 mM BDPA. The buildup curve was recorded with a melting time of 0.3 s and the melting curve was recorded with a 5 s polarization time.

3.2. ^{13}C DNP-NMR

In order to detect ^{13}C NMR spectra, a sample of 50 mM BDPA in pure ^{13}C-toluene was used for rapid-melt DNP. Besides an enhancement of the protons, the ^{13}C signal of the carbon labeled methyl group is enhanced by the rapid-melt DNP as well. A heteronuclear Overhauser mechanism transfers the hyperpolarization of the methyl protons to the methyl carbons [15]. In the frozen

state, the proton spins are hyperpolarized by DNP, which drives the ^{1}H polarization away from thermal equilibrium. Since methyl rotations are not quenched at liquid nitrogen temperatures, a cross-relaxation occurs between the methyl protons and the methyl carbon. Fig. 7 shows a carbon spectrum of a sample irradiated at 261.73 GHz, which corresponds to the solid effect frequency for protons. The proton enhancement in this experiment is lower than in the previous experiment ($\epsilon_{^{1}H} \approx -20$), which is caused by the lower radical concentration. Also, this sample does not contain deuterated toluene like in the previous experiment, which also affects the maximum enhancement that can be achieved [9].

Since BDPA is a narrow line radical, the direct DNP enhancement of ^{13}C is negligible. Interestingly, the enhancement of the carbons in the liquid state is large compared to the enhancement of the protons ($\epsilon_{^{13}C} \approx 60$). This relatively large carbon polarization is caused by the difference in relaxation rate between the protons and carbons. Due to the faster relaxation of protons during the melting and shuttling step, the final enhancement of the protons in the liquid state is attenuated.

Fig. 8 shows the DNP buildup curves of both the proton and carbon signal in this sample. The buildup time of the carbon polarization is significantly longer than that of the proton polarization, as the carbon spins are indirectly polarized by the proton spins.

3.3. Two-dimensional rapid-melt DNP-NMR

Since the sample composition does not change during the experiment, this rapid-melt DNP setup is well-suited for multidimensional NMR experiments. Here we demonstrate the application of rapid-melt DNP to 2D experiments using ethyl crotonate. Ethyl crotonate is often used to verify multidimensional experiments [16,17]. For this particular experiment, 500 mM ethyl crotonate was dissolved in deuterated toluene. To this mixture, approximately 50 mM BDPA radical was added.

Fig. 9 shows a COSY spectrum of this mixture with and without rapid-melt DNP. Both spectra were recorded accumulating 4 scans per t_1-increment recording 128 increments in total. The sample was hyperpolarized for 5 s and melted in 0.3 s (including shuttling). The resulting enhancement compared to a thermal spectrum was approximately -20. Due to variations in the final sample temperature, the DNP enhanced 2D spectrum has more t_1-noise compared to a thermal spectrum.

3.4. Heteronuclear rapid-melt DNP-NMR

Since the rapid-melt probe uses a double tuned stripline detector, it is also possible to perform heteronuclear 2D experiments. As a proof of concept, an HSQC experiment was performed on the sample of carbon labeled toluene from Section 3.2. Fig. 10 shows the resulting HSQC spectra. Both spectra were recorded accumulating 8 scans per increment, recording a total of 64 increments. The sample was hyperpolarized for 5 s and melted in 0.3 s (including shuttling). This resulted in an enhancement in the liquid state of approximately -20.

As the toluene is ^{13}C labeled at the methyl, only a single resonance is visible showing the correlation between the methyl carbon resonance and the methyl proton resonances. Carbon decoupling was not applied during acquisition, which results in a proton-carbon J-splitting being visible in the direct dimension.

4. Conclusions and outlook

In this manuscript, a 400 MHz rapid-melt DNP setup was presented, which is suitable for multidimensional and heteronuclear NMR experiments. With the rapid-melt technique, it is possible to obtain high liquid state enhancements by using an efficient solid state DNP mechanism. By melting the sample within the T_1 relaxation time, the loss of hyperpolarization during the phase transition is minimized. With this technique, enhancements of up to -175 have been observed for ^{1}H in low-concentration toluene in deuterated toluene.

When the methyl protons are hyperpolarized, their polarization transfers to the methyl carbon by a nuclear Overhauser effect, as shown in Section 3.2.

Since the sample composition does not change during the experiment, the rapid-melt DNP cycle can be repeated for signal averaging or for the acquisition of multidimensional spectra. This was demonstrated by recording a COSY spectrum of ethyl crotonate in toluene-d_8 with rapid-melt DNP enhancement. Also, a heteronuclear 2D spectrum using rapid-melt DNP has been recorded. In this case, an HSQC spectrum of ^{13}C-toluene was recorded. The rapid-melt DNP technique is quite general and can, in principle, be applied to most types of NMR experiments.

A remaining challenge with rapid-melt DNP is to improve on the stability of repeated experiments. Currently, the signal

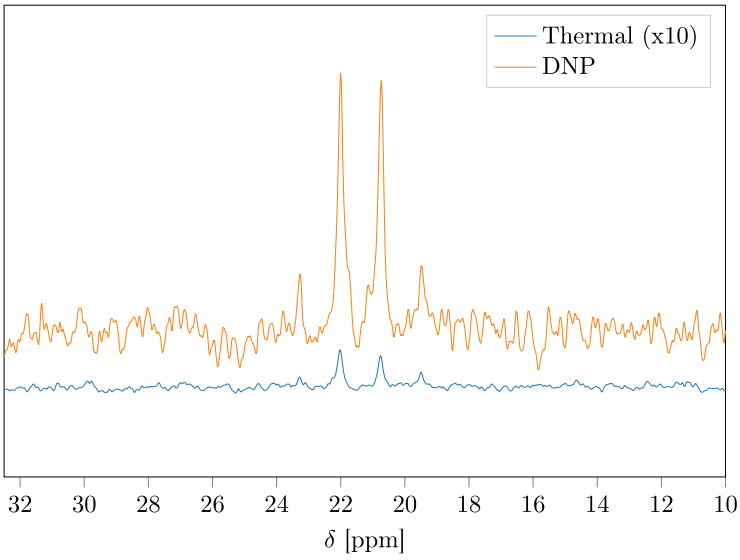

Fig. 7. The indirect DNP of carbon nuclei in ^{13}C-toluene with approximately 50 mM BDPA. The sample was polarized for 20 s and melted in 0.3 s. The DNP spectrum was recorded in a single scan. The thermal spectrum is an average of 256 scans.

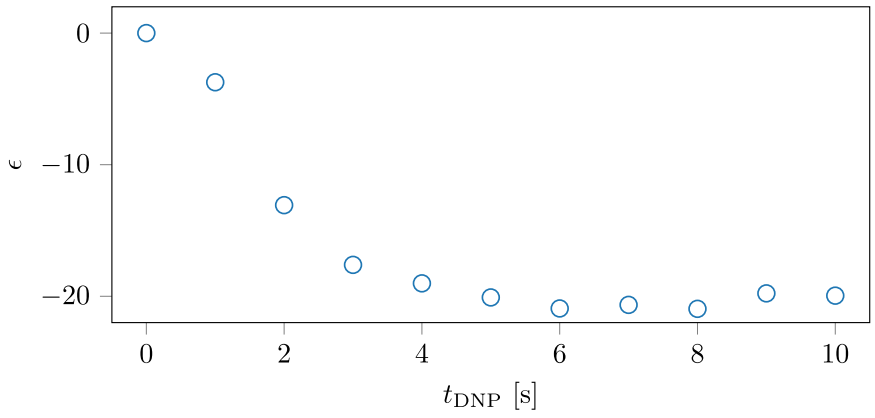

(a) Buildup curve ^{1}H

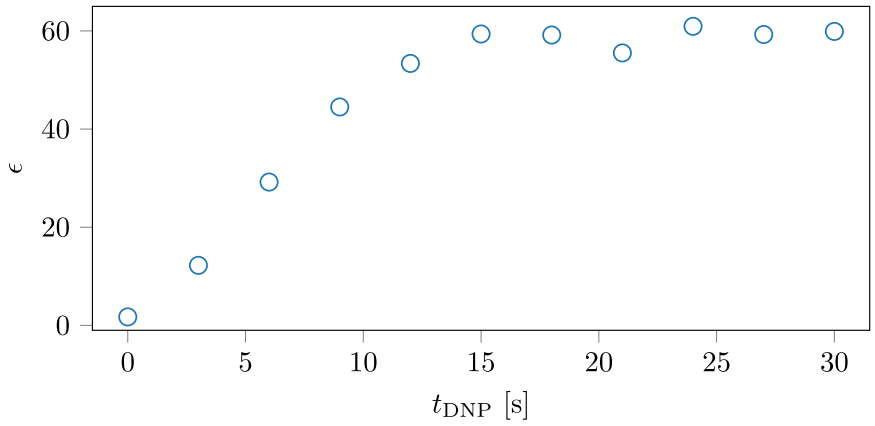

(b) Buildup curve ^{13}C

Fig. 8. The proton (a) and carbon (b) buildup curves of toluene (methyl ^{13}C) with approximately 50 mM BDPA radical. In both cases, the sample was irradiated with microwaves of 261.73 GHz (^{1}H solid effect).

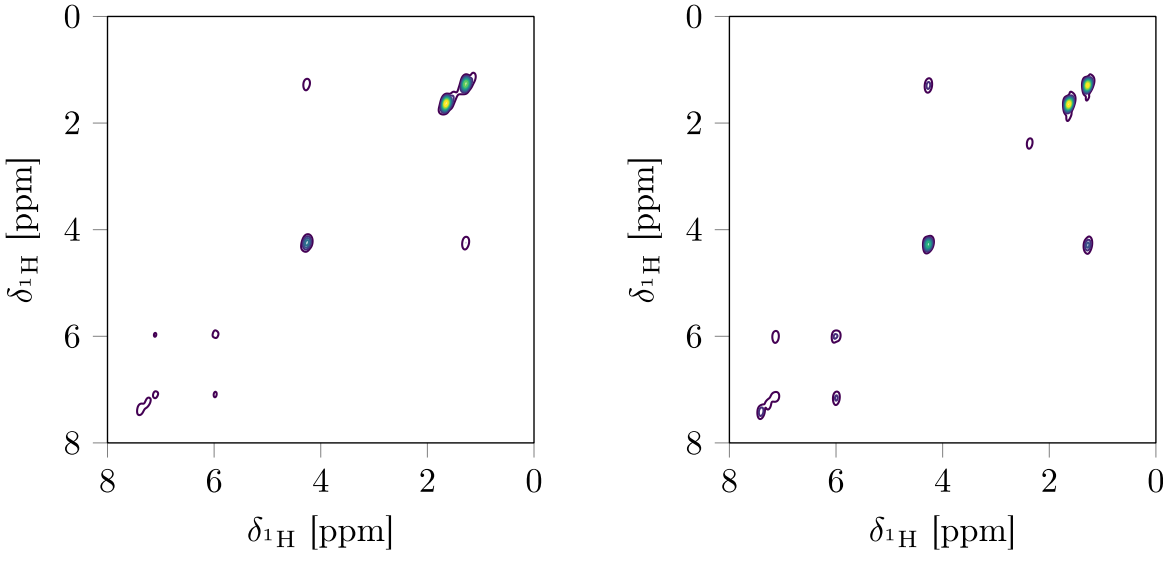

(a) Thermal

(b) Rapid-melt DNP

Fig. 9. COSY spectra of 500 mM ethyl crotonate in toluene-d_8 with approximately 50 mM BDPA. The spectra are recorded under thermal conditions (a) and with rapid-melt DNP enhancement (b).

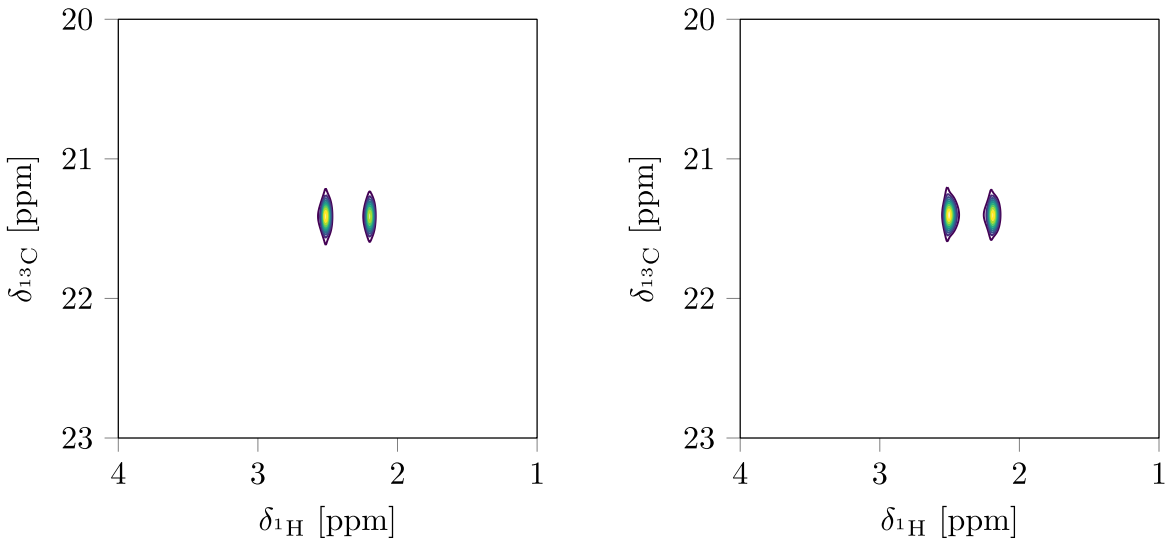

(a) Thermal (b) Rapid-melt DNP

Fig. 10. HSQC spectra of ^{13}C-toluene with approximately 50 mM BDPA. The spectra are recorded under thermal conditions (a) and with rapid-melt DNP enhancement (b).

intensity of the proton rapid-melt DNP varies between consecutive scans with a relative standard deviation of 2%. This is larger than the thermal noise as the DNP spectrum has an SNR of 950. This variation is an additional source of t_1-noise in 2D experiments and should be minimized. The main reason for the variations seems to be slight differences in the time it takes for the sample to melt, as the T_1 during melting depends strongly on the temperature of the sample. Efforts are being made to further improve the reproducibility of the melting. Another solution could be to implement Ultrafast experiments [18] and record complete 2D spectra in a single scan and use signal averaging to improve SNR.

The rapid-melt DNP technique is also applicable to stopped-flow experiments. For this purpose, a concentric capillary design was developed. When the capillary is in the NMR position, the entire sample is in the liquid state and can be replaced by a flow. This greatly improves throughput, since no interruption of the liquid nitrogen cooling is required and the probe does not need to be removed from the magnet to replace the sample. This way, it is possible to hyphenate the rapid-melt DNP to other techniques such as chromatography.

In this new rapid-melt DNP setup, it would also be possible to perform experiments where the sample is melted during the NMR sequence. For example, a sample could be hyperpolarized and moved to the stripline without melting the sample. Cross-polarization then transfers the large polarization of the proton spins to the carbon spins. The sample then moves down to the melt area and afterward moves back up to continue the NMR experiment in the liquid state. This method is of interest since the relaxation losses during melt are smaller for carbons than for protons. This means such a method could be preferred over a polarization transfer in the liquid state for samples with longer melting times (e.g., water) or for samples that require more exposed radicals (e.g., nitroxides). As was shown in previous research, the enhancements for TEMPOL-water samples are at least 3 times lower than BDPA-toluene at 95 GHz due to relaxation losses [12]. This is in contrast to the fact that the inhomogeneously broadened EPR resonance of TEMPOL is expected to result in more efficient solid-effect DNP. Repeated CP contacts have been shown to produce efficient hyperpolarization of carbon spins [19,20]. The advantage of this method is that no RF circuits are required inside the DNP area of the probe. The rapid-melt DNP setup is thus not limited in RF power by the presence of cryogens.

Acknowledgement

This research is funded by The Netherlands Organization for Scientific Research (NWO) in the framework of Technology Area COAST (053.21.115). The authors would also like to thank Jan van Bentum and Manvendra Sharma for their contributions to this project.

References

[1] T. Maly, G.T. Debelouchina, V.S. Bajaj, K.-N. Hu, C.-G. Joo, M.L. Mak-Jurkauskas, J.R. Sirigiri, P.C.A. van der Wel, J. Herzfeld, R.J. Temkin, R.G. Griffin, J. Chem. Phys. 128 (2008) 52211.
[2] J.H. Ardenkjaer-Larsen, B. Fridlund, A. Gram, G. Hansson, L. Hansson, M.H. Lerche, R. Servin, M. Thaning, K. Golman, Proc. Natl. Acad. Sci. 100 (2003) 10158.
[3] J.H. Ardenkjaer-Larsen, J. Magn. Reson. 264 (2016) 3.
[4] S.E. Day, M.I. Kettunen, F.A. Gallagher, D.-E. Hu, M. Lerche, J. Wolber, K. Golman, J.H. Ardenkjaer-Larsen, K.M. Brindle, Nat. Med. 13 (2007) 1382.
[5] P. Giraudeau, L. Frydman, Annu. Rev. Anal. Chem. (Palo Alto. Calif). 7 (2014) 129.
[6] C.-G. Joo, K.-N. Hu, J.A. Bryant, R.G. Griffin, J. Am. Chem. Soc. 128 (2006) 9428.
[7] C.-G. Joo, A. Casey, C.J. Turner, R.G. Griffin, J. Am. Chem. Soc. 131 (2009) 12.
[8] D. Yoon, M. Soundararajan, C. Caspers, F. Braunmueller, J. Genoud, S. Alberti, J.-P. Ansermet, J. Magn. Reson. 270 (2016) 142.
[9] M. Sharma, G. Janssen, J. Leggett, A. Kentgens, P. van Bentum, J. Magn. Reson. 258 (2015) 40.
[10] P.J.M. van Bentum, J.W.G. Janssen, a.P.M. Kentgens, J. Bart, J.G.E. Gardeniers, J. Magn. Reson. 189 (2007) 104.
[11] J. Bart, J.W.G. Janssen, P.J.M. van Bentum, a.P.M. Kentgens, J.G.E. Gardeniers, J. Magn. Reson. 201 (2009) 175.
[12] P.J.M. van Bentum, M. Sharma, S.G.J. van Meerten, a.P.M. Kentgens, J. Magn. Reson. 263 (2016) 126.
[13] S.G.J. van Meerten, P.J.M. van Bentum, A.P.M. Kentgens, Anal. Chem. 90 (2018) 10134.
[14] S. van Meerten, W. Franssen, A. Kentgens, J. Magn. Reson. 301 (2019) 56.
[15] D. Daube, V. Aladin, J. Heiliger, J.J. Wittmann, D. Barthelmes, C. Bengs, H. Schwalbe, B. Corzilius, J. Am. Chem. Soc. 138 (2016) 16572.
[16] S. Berger, S. Braun, 200 and more NMR Experiments, 2004, ISBN ISBN 3-527-31067-3.
[17] A.J. Oosthoek-de Vries, J. Bart, R.M. Tiggelaar, J.W.G. Janssen, P.J.M. van Bentum, H.J.G.E. Gardeniers, A.P.M. Kentgens, Anal. Chem. 89 (2017) 2296.
[18] L. Frydman, T. Scherf, A. Lupulescu, Proc. Natl. Acad. Sci. USA 99 (2002) 15858.
[19] M. Batel, M. Krajewski, A. Däpp, A. Hunkeler, B.H. Meier, S. Kozerke, M. Ernst, Chem. Phys. Lett. 554 (2012) 72.
[20] A. Bornet, A. Pinon, A. Jhajharia, M. Baudin, X. Ji, L. Emsley, G. Bodenhausen, J.H. Ardenkjaer-Larsen, S. Jannin, Phys. Chem. Chem. Phys. 18 (2016) 30530.